

Reliability of frontal sinus by cone beam-computed tomography (CBCT) for individual identification

Gianguido Cossellu¹ · Stefano De Luca^{2,5} · Roberto Biagi¹ · Giampietro Farronato¹ · Mariano Cingolani³ · Luigi Ferrante⁴ · Roberto Cameriere²

Received: 11 March 2015 / Accepted: 1 May 2015 / Published online: 16 May 2015
© Italian Society of Medical Radiology 2015

Abstract Analysis of the frontal sinus is an important tool in personal identification. Cone beam-computed tomography (CBCT) is also progressively replacing conventional radiography and multi-slice computed tomography (MSCT) in human identification. The aim of this study is to develop a reproducible technique and measurements from 3D reconstructions obtained with CBCT, for use in human identification. CBCT from 150 patients (91 female, 59 male), aged between 15 and 78 years, was analysed with the specific software program MIMICS 11.11 (Materialise N.V., Leuven, Belgium). Corresponding 3D volumes were generated and maximal dimensions along 3 directions (x , y , z), X_M , Y_M , Z_M (in mm), total volume area (in mm^3), V_t , and total surface (in mm^2), S_t , were calculated. Correlation analysis showed that sinus surfaces were strongly correlated with their volume ($r = 0.976$). Frontal sinuses were separate in 21 subjects (14 %), fused in 67 (44.6 %) and found on only one side (unilateral) in 9 (6 %). A Prominent Middle of Fused Sinus (PMS) was found in 53 subjects

(35.3 %). The intra- (0.963–0.999) and inter-observer variability (0.973–0.999) showed a great agreement and a substantial homogeneity of evaluation.

Keywords Forensic sciences · Human identification · Frontal sinus · Cone beam-computed tomography · Three dimensions · False negative

Introduction

Radiographic comparison of the frontal sinus is a well-recognized approach for reliable personal identification [1–8]. It has proven particularly useful when antemortem (AM) dental records are not available, when teeth are missing postmortem (PM), or in cases in which soft tissues are decomposed or burned [7–9].

Some typical features of frontal sinus morphology make it a very reliable part of the human skeleton for human identification [10]. The frontal sinus remains stable throughout an individual's life until old age, when progressive pneumatization due to atrophic changes may occur [11–14]. The frontal sinus is also preserved intact as its internal bony structure protects it from injury [15–18]. Lastly, it is highly variable in nature and shows differences even between monozygotic twins [16], as demonstrated by several radiographs, among which researchers could not find two identical ones [19, 20].

AM and PM radiographs of the frontal sinuses can be compared by overlapping or coding systems [18, 21]. Overlapping is accepted as a reliable method but it does cause some problems which are overcome by coding systems [22–25].

In spite of the large number of publications relating to the uniqueness of frontal sinuses, there is a real need for more research aimed at quantification [25]. As Christensen

✉ Stefano De Luca
sluca@ugr.es

¹ Department of Biomedical, Surgical and Dental Sciences, Unit of Orthodontics and Pediatric Dentistry, University of Milan, Fondazione IRCCS Cà Granda Ospedale Maggiore Policlinico, Milan, Italy

² AgEstimation Project, Institute of Legal Medicine, University of Macerata, Macerata, Italy

³ Institute of Legal Medicine, University of Macerata, Macerata, Italy

⁴ Department of Biomedical Sciences and Public Health, Faculty of Medicine, Polytechnic University of Marche, Ancona, Italy

⁵ Calle las moreras 77, 28971 Griñón, Madrid, Spain

stated [20, 25], although many claim that the frontal sinuses are unique to each individual, no empirical studies have ever rigorously tested this statement.

Some recent publications have stressed the possibility of studying frontal sinuses by computed tomography (CT) [26–29]. These techniques provide very good opportunities for studying these anatomical structures with a three-dimensional approach and great precision in all measurements [30]. They also present several advantages over conventional radiographs: superimposition of structures beyond the plane of interest can be avoided, allowing visualization of small differences in density [26, 27, 29]; internal points for evaluation can be easily shown by image segmentation; craniometric points can be precisely located and measurements more accurately performed than on conventional radiographs. Hence, volumes and areas can be determined [27, 28, 31].

Cone beam-computed tomography (CBCT) has recently begun to emerge as a potentially low-dose cross-sectional technique for visualizing bony structures in the head and neck [26, 30]. The technology involves a cone-shaped X-ray beam directed at a flat two-dimensional (2D) detector. As both rotate around the subject's head, a series of 2D images are generated. The software can then apply a particular algorithm to reconstruct the images into a three-dimensional (3D) dataset [32].

Comparatively low dosing requirements, high-quality bony definition and the compact design afforded by CBCT scanners have made them attractive for office-based and intra-operative scanning of frontal sinuses [32]. Radiation dose is very important because in the field or non-specific location, such as a laboratory, shielding operators are essential [33]. Last but not least, its portability makes it ideally suited to field use. The machine can be transported and easily positioned in place like a cart, allowing its use on virtually any levelled temporary facility [33].

In this context, the most commonly used techniques are based on evaluation of both metric and non-metric characteristics of frontal sinus patterns. For example, in 1987, Yoshino et al. [19] proposed a system of classification based on the following morphological characteristics: area size, bilateral asymmetry, superiority of area size, outline of superior borders, partial septa and supra-orbital cells were collected and classified with code numbers. The authors state that the possibility of having the same code for two different individuals is one every 23,040 cases.

In 2005, to improve the performance of the above method for individual identification, Cameriere et al. [34] proposed a new system of classification based on the following morphological characteristics: ratio between left frontal sinus area and left orbital area (SOR_1) and ratio between right frontal sinus area and right orbital area (SOR_2), instead of the area size and bilateral asymmetry of

Yoshino's method. Cameriere et al. [24] also attempted to estimate the probability of misclassification.

With the above methods, the probability of making a positive identification error (i.e. the probability of identifying two images of two different skulls as belonging to the same person) was found to be 1/20,000 by Yoshino et al. [19] and $p < 10^{-6}$ by Cameriere et al. [24].

The aim of the present study was to develop a reproducible technique and measurements from 3D reconstructions obtained with CBCT, for human identification purposes.

Materials and methods

CBCT scans of 150 patients (91 female, 59 male), aged between 15 and 78 years, were selected from those treated at the Unit of Orthodontics and Pediatric Dentistry, University of Milan (Italy).

All these examinations were performed with the same CBCT unit: i-CAT (Imaging Sciences International, Hatfield, PA) and the same settings: 120 kV and 20 mA. The scanning protocol involved 0.4-mm slice thickness, 16×22 cm field of view, 20-second scan time and 0.4 mm voxel size.

Inclusion criteria were as follows: patients had at least one frontal sinus; they were at least 15-years old; they had had i-CAT (Imaging Sciences International, Hatfield, PA, USA) CBCT scans previously, for planned orthodontic treatment; and their sinuses were not inflamed and not involved in any systemic disease.

The raw data were saved in DICOM format and then imported into the specific software program MIMICS 11.11 (Materialise N.V., Leuven, Belgium). Reconstruction of the coronal ($x-z$), sagittal ($y-z$) and transversal ($x-y$) planes were analysed.

According to the minimal and maximal threshold values, one layer of the relevant structures (airways) was called the mask, and was defined and colour-coded. Air has the lowest values of HU (Hounsfield Unit) and while bone has the highest. Threshold levels for air were therefore determined for all CBCT datasets, in this case HU from -1024 to -20 . Because of the connection of the air to the surroundings, pixel need to be erased with mask editing so the field of view can be excluded from the surroundings. When all the connections are broken, new pixels are added inside the volume for the whole volume to be measured. When the sinus is air filled, the only procedure needed is selecting the mask by thresholding air and then use the tool dilate for 2–3 pixels (Fig. 1a, b).

Its corresponding 3D volume was then generated through the voxel size and number of voxels in the 3D object (Fig. 2). The contour interpolation algorithm is used to visualize the 3D model of the frontal sinus and the grey

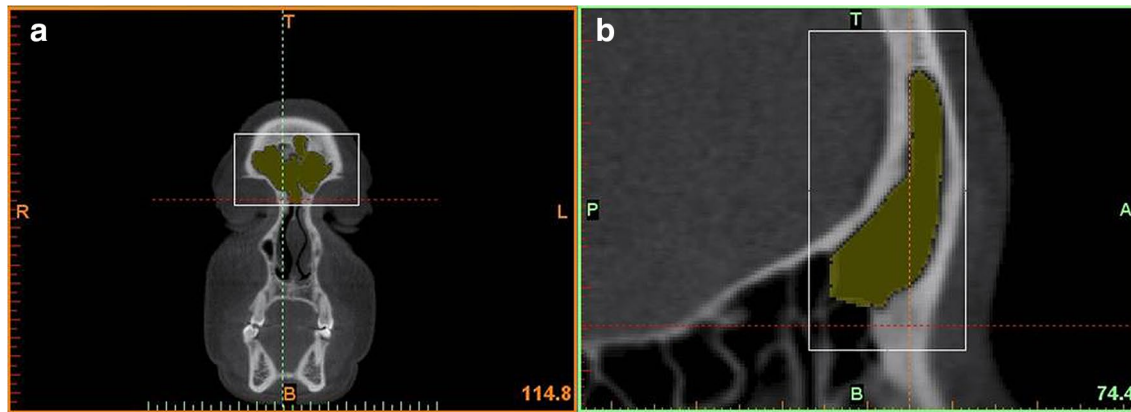


Fig. 1 a, b Coronal (frontal) and mid-sagittal (lateral) views during the isolation of the frontal sinus (evidenced in yellow). The coronal section (a) is approximately at the premolar level. Mid-sagittal sec-

tion (b) is best for the evaluation of the visible portion of the airway. This section can be generated with simple functions using the CBCT scanner's software applications

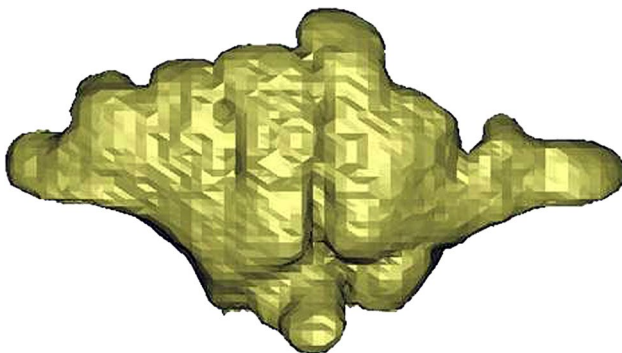


Fig. 2 3D volume rendering of the frontal sinus

interpolation algorithm to calculate and measure the sinus volume.

On the basis of this reconstruction, maximal dimensions along 3 directions (x , y , z), X_M , Y_M , Z_M (in mm), total volume area (in mm^3), V_t , and total surface (in mm^2), S_t , were calculated on the whole structure of the frontal sinuses.

The line drawn parallel to the Frankfort horizontal plane and passing through the tightest area of the sinus before its connection with the nose and the lower airway was chosen as the baseline of the sinus (Fig. 1) as a reference limit, in order to determine the whole volume of the sinuses which sometimes could not be significantly isolated if the baseline was drawn in an area above. All nonmetric characteristics and metric measurements were recorded after the frontal sinus was cut from the baseline. This choice is also one which may cause operators to make minor but statistically insignificant differences when volume sizes are measured.

Protocols to collect CBCT images for human subjects were approved by the Ethics Committee for Research Involving Human Subjects of the University of Milan (Italy), and the study was conducted in accordance with the

ethical standards laid down by the Declaration of Helsinki (Finland). The World Medical Association (WMA) developed the Declaration of Helsinki as a statement of ethical principles for medical research involving human subjects, including research on identifiable human material and data.

To test intra-observer reliability, a random sample of 30 CBCT scans were each re-examined twice, at two-week intervals. Assessment of inter-observer reliability was carried out by two observers, each of whom evaluated 30 randomly selected CBCT scans.

Randomly selected means that each scan among the analysed CBCT has an equal and independent chance of being selected to belong to the sample of 30 CBCT scans used to test reliability of the method. Effectively, the function “sample” of the statistical environment R has been used to take a sample of 30 scans from 150 numbered CBCT.

Intra- and inter-observer reliability was studied with the intra-class correlation coefficient (ICC) [35, 36].

Statistical analysis

In this preliminary study, only the quantitative variables characterizing 3D frontal sinus patterns were analysed. Descriptive statistics were performed for variables X_M , Y_M , Z_M , V_t and S_t . In particular, correlation analysis was carried out among all these variables, to find the least correlated ones, i.e. those with correlation coefficient r such that $|r| < 0.9$.

Six quantitative variables (parameters) measured have been taken for each skull: maximal dimensions of sinuses along 3 directions (x , y , z), X_M , Y_M , Z_M (in mm), total volume area (in mm^3), V_t , and total surface (in mm^2), S_t , of the whole structure of the frontal sinuses. If two of these variables were strongly correlated, the information acquired

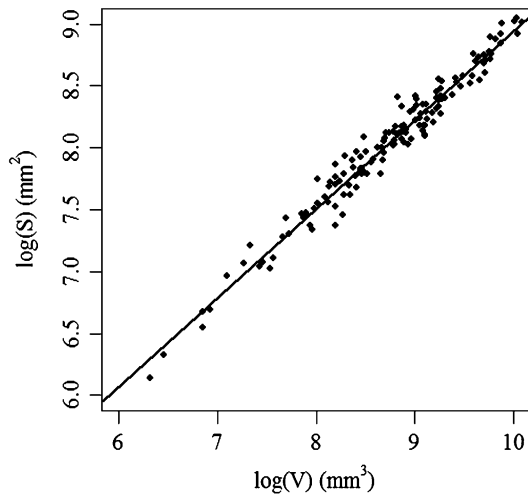


Fig. 3 Simple linear regression between the logarithm of S_t and the logarithm of V_t

considering one of them should not differ from that acquired using both variables. For example, in this study, a simple linear regression between the logarithm of S_t and the logarithm of V_t points out that 97 % of the variability of S_t can be explained by the variability of V_t (Fig. 3). Consequently, it is not useful for the identification process to consider both variables. The choice to include V_t and to remove S_t is related to the variability among subjects of V_t which is greater than the variability of S_t .

Once the variables considered for individual identification by frontal sinus had been selected, the re-examined CBCT scans were used to assess the intra-observer variability of the chosen statistical variables. Within-subject variability was characterized by assuming that it was only due to errors on repeated measurements of the same scan, and that these errors were normally distributed.

The tolerance region at level $1-\alpha$ for each individual was then evaluated. This region consists of measurement vectors x satisfying:

$$(x - \mu)' \sum^{-1} (x - \mu) \leq \chi_k^2(1 - \alpha) \tag{1}$$

where x is a k -dimensional vector of measurements of a 3D frontal sinus pattern chosen for identification, μ is the known k -dimensional vector of measurements of a 3D frontal sinus pattern in the given individual and \sum is the estimated covariance matrix associated with within-subject variability due to inter-observer error measurement. Lastly, $\chi_k^2(1 - \alpha)$ indicates the quantile function for probability $1-\alpha$ of the Chi squared distribution, with k degrees of freedom. That is, if a k -dimensional vector of measurement of a 3D frontal sinus pattern, x , is located out of the region of tolerance with centre μ , it does not refer to the same

individual characterized by μ , with a probability of a false-negative error of less than α .

Calculation of probability of individual identification

In order to estimate the tolerance region at level $(1-\alpha) = 95 \%$, the re-examined observations (30 subjects) were used to determine inter-observer variability by assessing the covariance matrix:

$$\sum = \begin{pmatrix} 0.13 & 0.23 & 0.26 & 26.91 \\ 0.23 & 1.34 & 0.50 & 73.18 \\ 0.26 & 0.50 & 0.80 & 63.96 \\ 26.91 & 73.18 & 63.96 & 7843.11 \end{pmatrix} \tag{2}$$

Entering covariance matrix (2) in inequality (1) yielded the tolerance region at level 95 %. For example, if we know that a subject has $X_M = 49.89$ mm, $Y_M = 25.74$ mm, $Z_M = 33.60$ mm and $V_t = 9011.95$ mm³, then the centre of tolerance region for that subject is $\mu = (49.89, 25.74, 33.60, 9011.95)$.

Subsequently, another CBCT scan of the frontal sinuses of an unknown subject was compared with the following measures: $X_M = 50.89$ mm, $Y_M = 26.74$ mm, $Z_M = 34.60$ mm and $V_t = 9111.95$ mm³. The question for identification was “Does the second CBCT scan belong to the same subject?” According to inequality (1), since the first term $(x - \mu)' \sum^{-1} (x - \mu) = 15.06$ is not less than the second term $\chi_k^2(1 - \alpha) = 9.49$, the second CBCT scan does not belong to the tolerance region of the same subject. This means that the second subject is different from the first one, with a probability $\alpha = 5 \%$ of erroneously rejecting the hypothesis that the two scans belong to the same subject. The distribution of the logarithm of the Mahalano-bis distance among the 150 scans is shown in Fig. 4.

Results

Frontal sinuses were separate in 21 subjects (14 %), fused in 67 (44.6 %) and found on only one side (unilateral) in 9 (6 %). A prominent middle of fused sinus (PMS) was found in 53 subjects (35.3 %) (Table 1).

Correlation analysis (Table 2) showed that sinus surfaces were strongly correlated with their volume ($r = 0.976$). Consequently, S_t was excluded from the variables used in the identification procedure, because it carried a very small amount of information with respect to that obtained from the other four variables. Hence, each subject was identified according to the four variables X_M, Y_M, Z_M and V_t .

As regards the intra-observer variability of X_M, Y_M, Z_M and V_t measurements, ICC ranged between 0.963 and

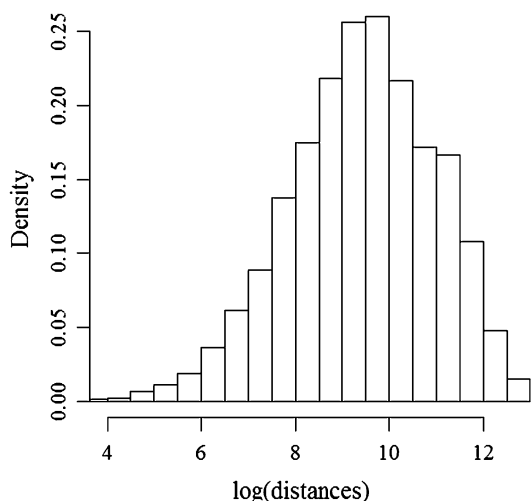


Fig. 4 Distribution of the logarithm of the Mahalanobis distance among the 150 skulls

Table 1 Asymmetry of frontal sinuses in the Italian sample according to gender

Gender	Fused	Left only	Right only	PMS	Separated
Male	30	2	3	17	8
Female	37	2	2	36	13
Total	67	4	5	53	21

PMS prominent middle sinus (22)

Table 2 Correlation among five quantitative variables, calculated on whole structure of sinuses

	X_M	Y_M	Z_M	V_t	S_t
X_M	1.000	0.545	0.813	0.850	0.904
Y_M	0.545	1.000	0.484	0.714	0.715
Z_M	0.813	0.484	1.000	0.805	0.864
V_t	0.850	0.714	0.805	1.000	0.976
S_t	0.904	0.715	0.864	0.976	1.000

0.999. Regarding the inter-observer variability of the same measurements, ICC ranged from 0.973 to 0.999, and did not reveal significant intra- or inter-observer effects, indicating substantial homogeneity of evaluation.

Discussion

In recent years, the increase and improvements in 3D radiographic techniques (MRI and CT) have generated so many data that they can also be used for identification purposes. Compared with traditional 2D techniques, 3D images yield

far more information. In addition to data from the coronal plane with traditional X-rays, CBCT scanning allows assessment of sinus depth, area and volume. In the last few years, self-shielded CBCT machines have also reduced radiation, compared with multi-slice CT (MSCT) scanning and conventional radiography; its relative low cost make acquisition more feasible; it can be also used in a wider range of subjects, and easily transported and operated for either office or mobile morgues [37, 38]. Lastly, the CBCT machines are user-friendly and limited training is necessary to use them. Although CBCT has not yet gained wide acceptance in forensic community, Sarment and Christensen encourage its use for many forensic applications [33].

In this study, frontal sinuses were separate in 21 subjects (14 %), fused in 67 (44.6 %) and found on only one side (unilateral) in 9 (6 % total, 2.6 % in females and 3.4 % in males). A PMS was found in 53 subjects (35.3 %, 11.3 in males and 24.6 in females). Because the left and right frontal sinuses develop independently, a significant asymmetry between these sinuses can arise in the same individual [39]. Occasionally, one or both sinuses may be absent. Yoshino et al. [19] reported the frequency of a unilateral sinus absence as 13.3 % for males and 16.9 % in females. The frequency of frontal sinus agenesis is variable between different populations [40].

The term fused sinus is used here to describe adjoining of the right and left sinuses [19]. Prominent middle sinus was defined as the attachment of both sinuses: one sinus overdeveloped, with the middle of the fused sinus protruding [19]. The fused and prominent middle sinuses were the highest types in this study. In Yoshino et al. [19], the frequency of the fused and prominent middle sinus was 53 % in males and 34 % in females. In Lee et al. [41], the frequency was 66.9 % in males and 60.2 % in females. Although the fused and prominent middle sinuses were not mentioned in previous studies, their importance should be taken into account when the frontal sinus is classified by morphology.

Concerning the intra- and inter-observer variability, ICC ranged between 0.963 and 0.999 and between 0.973 and 0.999, respectively. These results showed a strong agreement for the same reader and also between different operators with high accuracy. The high agreement renders frontal sinus identification system to be a simple method for establishing the identification of unknown persons for whom frontal sinus X-rays exist.

Of the variables considered for identification purposes, total surface (S_t) was not used in this study because it is highly correlated with volume ($r = 0.976$) and therefore does not increase the quantity of identifying information.

Each CBCT scan corresponds to a point, P , in the four-dimensional space identified by X_M , Y_M , Z_M and V_t .

Measured distances are quantitative characteristics and may vary, depending on manual reconstruction of the images, so it was concluded that one and the same skull always show an identical value for a certain measured parameter. Consequently, for identification purposes, the variability of CBCT measurements was considered and assessed in the frontal sinuses of the same subject. In this respect, one of the main aims of this paper was to evaluate, in each individual, the tolerance region, i.e. the 4D region T , where each point corresponds to the same subject. Conversely, a point which does not belong to this region represents a different subject, with a small fixed probability, α , of yielding a false-negative error.

As regards the probability of obtaining a positive identification error, i.e. two different subjects belong to the same tolerance region, none of the 150 individuals in this sample fell in the tolerance region of another individual.

Conclusions

The technique described in this study could increase the usefulness of the frontal sinus identification method in new forms of 3D examinations such as CBCT. The comparison of frontal sinus images by CBCT can be used as an additional method in the identification process, providing the expert with greater reliability. Forensic researchers are expected to achieve more numerous identifications in the future by applying CBCT scanning.

Acknowledgments The authors would like to thank the staff of the Unit of Orthodontics and Pediatric Dentistry, University of Milan (Italy) for their assistance on this project, and also Ms. Gabriel Walton for editing the English text. Thanks also to the editor and the reviewers for helpful comments that have improved this paper.

Conflict of interest The authors declare that they have no conflict of interest.

Ethical standards All procedures performed in studies involving human participants were in accordance with the ethical standards of the institutional and/or national research committee and with the 1964 Helsinki declaration and its later amendments or comparable ethical standards.

Informed consent Informed consent was obtained from all individual participants included in the study.

References

- David MP, Saxena R (2010) Use of frontal sinus and nasal septum patterns as an aid in personal identification: a digital radiographic pilot study. *J Forensic Dent Sci* 2:77–80
- Kanchan T, Krishan K, Menezes RG, Suresh Kumar Shetty B, Lobo SW (2010) Frontal sinus radiographs—a useful means of identification. *J Forensic Leg Med* 17:223–224
- Tatlisumak E, Asirdizer M, Sunay Yavuz M (2011) Usability of CT Images of frontal sinus in forensic personal identification. In: Homma N (ed) *Theory and applications of CT imaging and analysis*. InTech, Rijeka, pp 257–268
- Abraham J, Champod C, Lennard C, Roux C (2013) Spatial analysis of corresponding fingerprint features from match and close non-match populations. *Forensic Sci Int* 230(1–3):87–98
- Schuliar Y, Knudsen PJ (2012) Role of forensic pathologists in mass disasters. *Forensic Sci Med Pathol* 8:164–173
- Schwark T, Heinrich A, Von Wurmb-Schwark N (2011) Genetic identification of highly putrefied bodies using DNA from soft tissues. *Int J Legal Med* 125:891–894
- Rios L, García-Rubio A, Martínez B, Alonso A, Puente J (2012) Identification process in mass graves from the Spanish Civil War II. *Forensic Sci Int* 219:e4–e9
- Ishii M, Yayama K, Motani H, Sakuma A, Yasjima D, Hayakawa M, Yamamoto S, Iwase H (2011) Application of superimposition-based personal identification using skull computed tomography images. *J Forensic Sci* 56:960–966
- Berketa JW (2014) Maximizing postmortem oral-facial data to assist identification following severe incineration. *Forensic Sci Med Path* 10(2):208–216
- Patil N, Karjodkar FR, Sontakke S, Sansare K, Salvi R (2012) Uniqueness of radiographic patterns of the frontal sinus for personal identification. *Imaging Sci Den* 42:213–217
- McLaughlin RB Jr, Rehl RM, Lanza DC (2001) Clinically relevant frontal sinus anatomy and physiology. *Otolaryng Clin N Am* 34:1–22
- Seiden AM (2005) Frontal headache. In: Kountakis SE, Senior BA, Draf W (eds) *The frontal sinus*. Springer, Berlin, pp 115–126
- Allen BC (1961) Applied anatomy of paranasal sinuses. *J Am Osteopath Assoc* 60:978
- Kirk NJ, Wood RE, Goldstein M (2002) Skeletal identification using the frontal sinus region: a retrospective study of 39 cases. *J Forensic Sci* 47:318–323
- Cox M, Malcolm M, Fairgrieve SI (2009) A new digital method for the objective comparison of frontal sinuses for identification. *J Forensic Sci* 54:761–772
- Nambiar P, Naidu MD, Subramaniam K (1999) Anatomical variability of the frontal sinuses and their application in forensic identification. *Clin Anat* 12:16–19
- Wallis A, Donal PJ (1988) Frontal sinus fractures: a review of 72 cases. *Laryngoscope* 98:593–598
- Quatrehomme G, Fronty P, Sapanet M, Grévin G, Bailet P, Ollier A (1996) Identification by frontal sinus pattern in forensic anthropology. *Forensic Sci Int* 83:147–153
- Yoshino M, Miyasaka S, Sato H, Seta S (1987) Classification system of frontal sinus patterns by radiography. Its application to identification of unknown skeletal remains. *Forensic Sci Int* 34:289–299
- Christensen AM (2004) The impact of *Daubert*: implications for testimony and research in forensic anthropology (and the use of frontal sinuses in personal identification). *J Forensic Sci* 49(3):1–4
- Campobasso CP, Dell’erba AS, Belviso M, Di Vella G (2007) Craniofacial identification by comparison of antemortem and postmortem radiographs: two case reports dealing with burnt bodies. *Am J Forensic Med Pathol* 2:182–186
- Ribeiro Fde A (2000) Standardized measurements of radiographic films of the frontal sinuses: an aid to identifying unknown persons. *Ear Nose Throat J* 79:26–33
- Tatlisumak E, Ovali GY, Aslan A, Asirdizer M, Zeyfeoglu Y, Tarhan S (2007) Identification of unknown bodies by using CT images of frontal sinus. *Forensic Sci Int* 166:42–48
- Cameriere R, Ferrante L, Molleson T, Brown B (2008) Frontal sinus accuracy in identification as measured by false positives in kin groups. *J Forensic Sci* 53:1280–1282

25. Christensen AM (2005) Assessing the variation in individual frontal sinus outlines. *Am J Phys Anthropol* 127:291–295
26. Kim DI, Lee UY, Park SO, Kwak DS, Han SH (2012) Identification using frontal sinus by three-dimensional reconstruction from computed tomography. *J Forensic Sci* 58(19):5–12
27. Jackowski C, Wyss M, Persson A, Classens M, Thali MJ, Lussi A (2008) Ultra-high-resolution dual-source CT for forensic dental visualization-discrimination of ceramic and composite fillings. *Int J Legal Med* 122(43):301–307
28. Carvalho SPM, Alves da Silva RH, Lopes-Júnior C, Peres AS (2009) Use of images for human identification in forensic dentistry. *Radiol Bras* 42(2):125–130
29. Uthman AT, Al-Rawi NH, Al-Naaimi AS, Tawfeeq AS, Suhail EH (2010) Evaluation of frontal sinus and skull measurements using spiral CT scanning: an aid in unknown person identification. *Forensic Sci Int* 197(124):e1–e7
30. Cappabianca S, Perillo L, Esposito V, Iaselli F, Tufano G, Thanassoulas TG et al (2013) A computed tomography-based comparative cephalometric analysis of the Italian craniofacial pattern through 2,700 years. *Radiol Med* 118(2):276–290
31. Reichs KJ (1993) Quantified comparison of frontal sinus patterns by means of computed tomography. *Forensic Sci Int* 61:141–168
32. Miracle AC, Mukherji SK (2009) Cone-beam CT of the head and neck, Part 2: clinical applications. *Am J Neuroradiol* 30:1285–1292
33. Sarment D, Christensen AM (2014) The use of cone beam computed tomography in forensic radiology. *J Forensic Rad Imag* 2(4):173–181
34. Cameriere R, Ferrante L, Mirtella D, Rollo FU, Cingolani M (2005) Frontal sinuses for identification: quality of classifications, possible error and potential corrections. *J Forensic Sci* 50(4):770–773
35. Ferrante L, Cameriere R (2009) Statistical methods to assess the reliability of measurements in the procedures for forensic age estimation. *Int J Legal Med* 123:277–283
36. Shrout PE, Fleiss JL (1979) Intra-class correlations: uses in assessing rater reliability. *Psychol Bull* 2:420–428
37. Kapila S, Conley RS, Harrell WE Jr (2011) The current status of cone beam computed tomography imaging in orthodontics. *Dentomaxillofac Rad* 40:24–34
38. Besana JL, Rogers TL (2010) Personal identification using the frontal sinus. *J Forensic Sci* 55:584–589
39. Levine HL, Clemente MP (2003) Surgical anatomy of the paranasal sinus. In: Clemente MP (ed) *Sinus surgery: endoscopic and microscopic approaches*. Thieme, Stuttgart, pp 1–55
40. Shah RK, Dhingra JK, Carter BL, Rebeiz EE (2003) Paranasal sinus development: a radiographic study. *Laryngoscope* 113:205–209
41. Lee HK, Kwon KH, Kim KJ, Kang SM, Moon GJ (1985) A study on the classification of frontal sinuses and distributions using simple AP skull radiographies. *J Soonchunhyang Univ* 8(4):481–485